Electronic Supplementary Material (ESI) for Journal of Materials Chemistry C.

Facile Large-Scale Synthesis of Monodisperse REF_3 (RE=Y, Ce, Nd, Sm-Lu) Nano/Microcrystals and Luminescence Properties

*Baiqi Shao, Qi Zhao, Yongchao Jia, Wenzhen Lv, Mengmeng Jiao, Wei Lü and Hongpeng You**

State Key Laboratory of Rare Earth Resource Utilization, Changchun Institute of Applied Chemistry, Chinese Academy of Sciences, Changchun 130022, and Graduate University of the Chinese Academy of Sciences, Beijing 100049, P. R. China

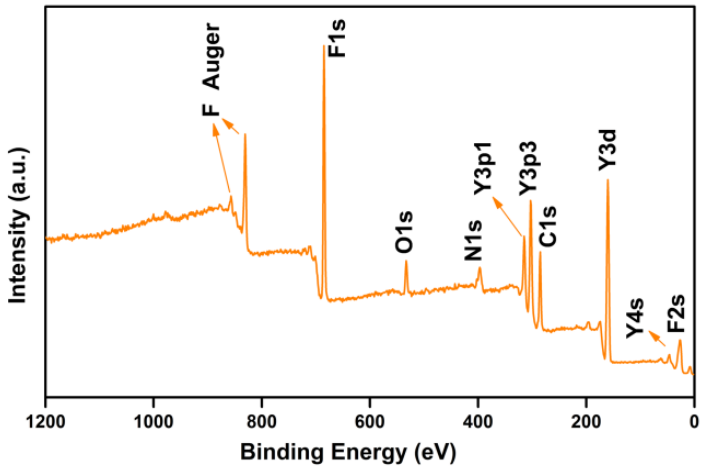

Figure S1 The XPS spectrum of the as-prepared $YF_3 \cdot xNH_4F \cdot yH_2O$ precursors.

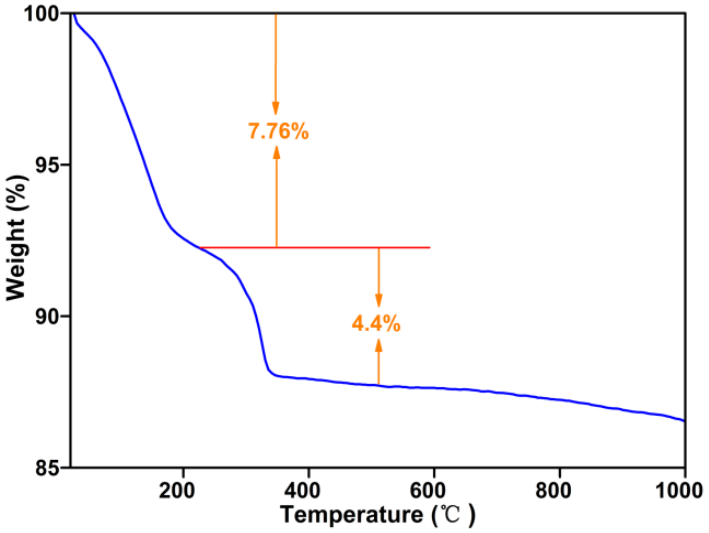

Figure S2 The TGA curve of the as-prepared $YF_3 \bullet xNH_4F \bullet yH_2O$ precursors.

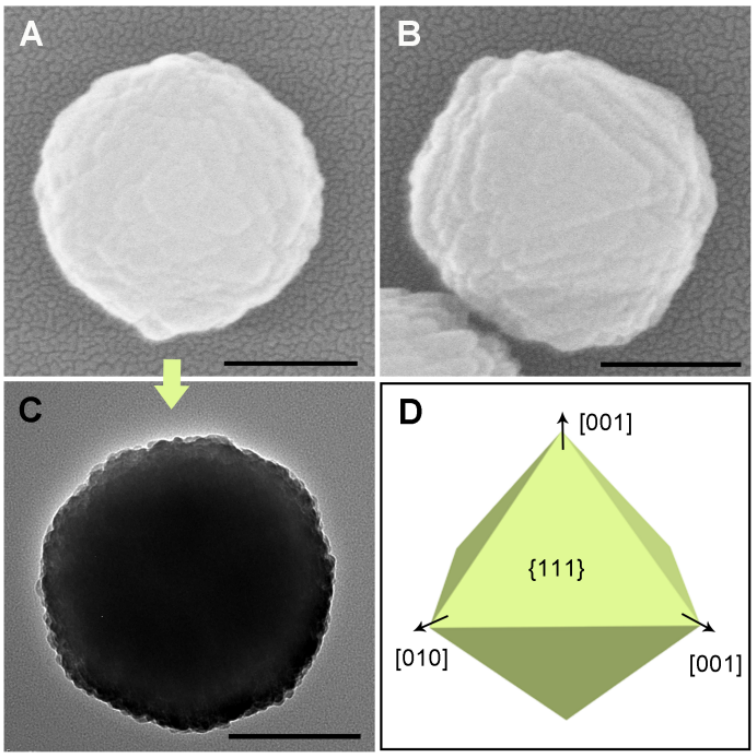

Figure S3 The SEM (A and B, from different angle of view), TEM (C) images, and the schematic illustration of the individual particle. The scale bar is 200 nm.

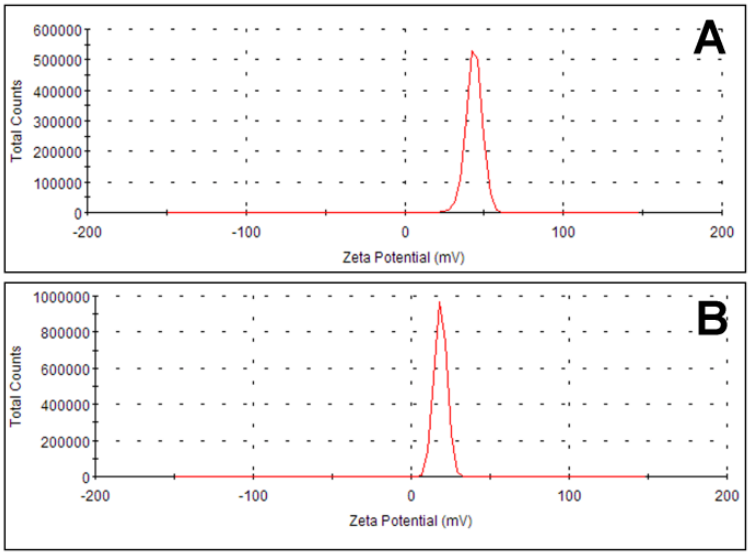

Figure S4 The zeta potential curves of the suspension liquid before (A) and after (B) ammonia adding.

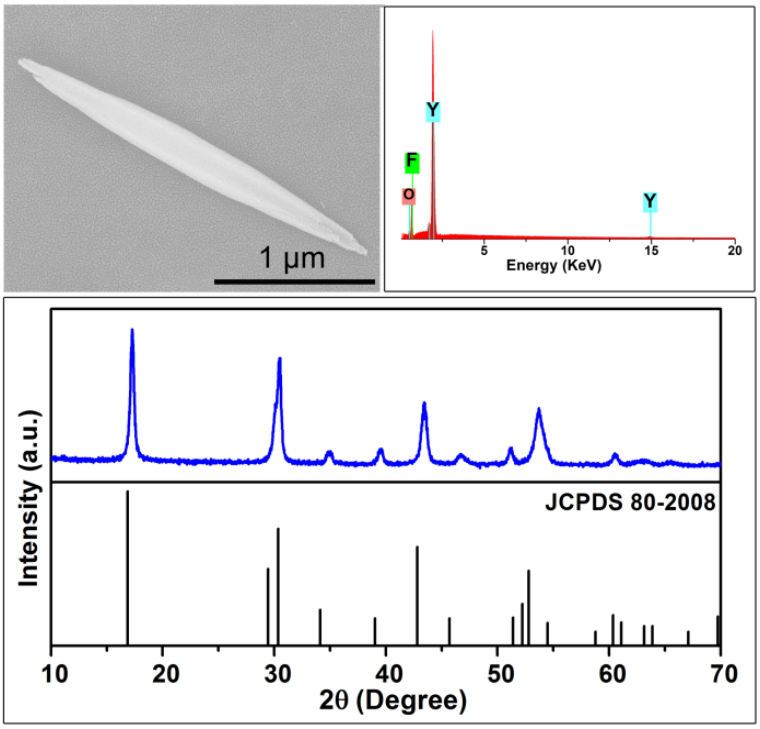

Figure S5 The magnified SEM image, EDX spectrum, and XRD pattern of the $Y(OH)_xF_{3-x}$ microstructure. The standard XRD pattern cannot be found in the database, and the pattern is closes to $Y(OH)_{1.57}F_{1.43}$ (JCPDS No. 80-2008). The EDX spectrum confirms the presences of Y, O, and F elements in the sample.

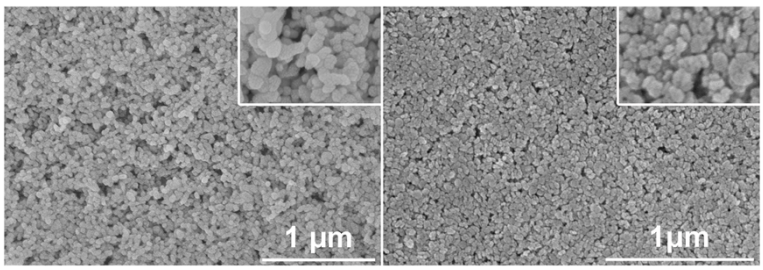

Figure S6 SEM image of the as-prepared LaF_3 and PrF_3 products.

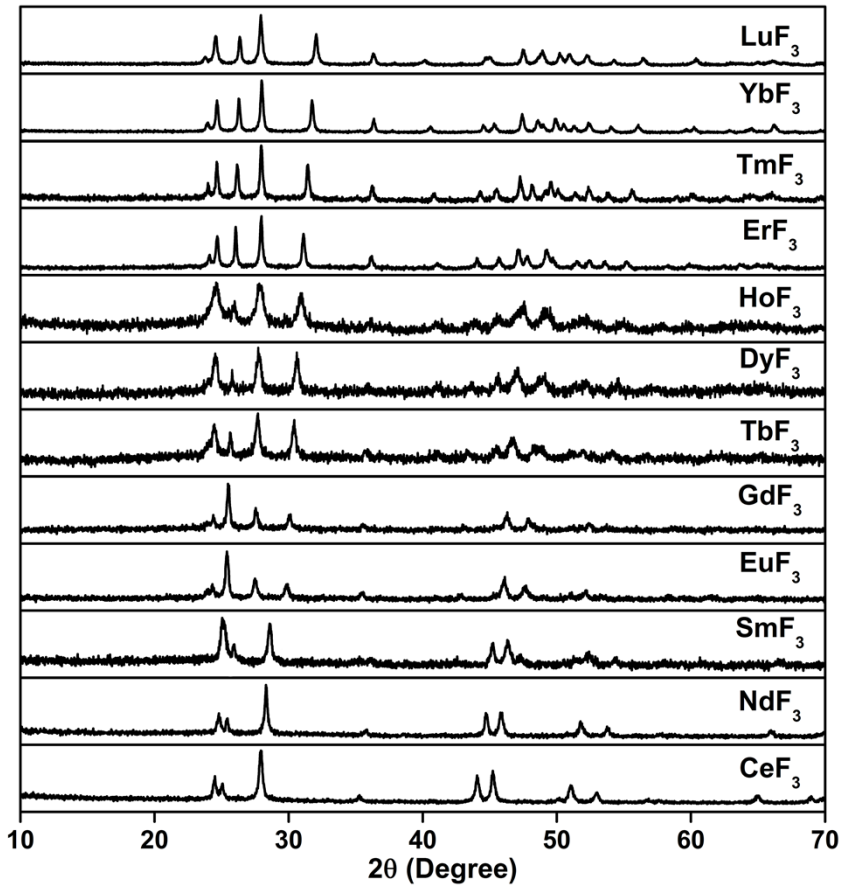

Figure S7 The XRD patterns of the as-prepared REF_3 (RE = Ce, Nd, Sm-Lu) products.

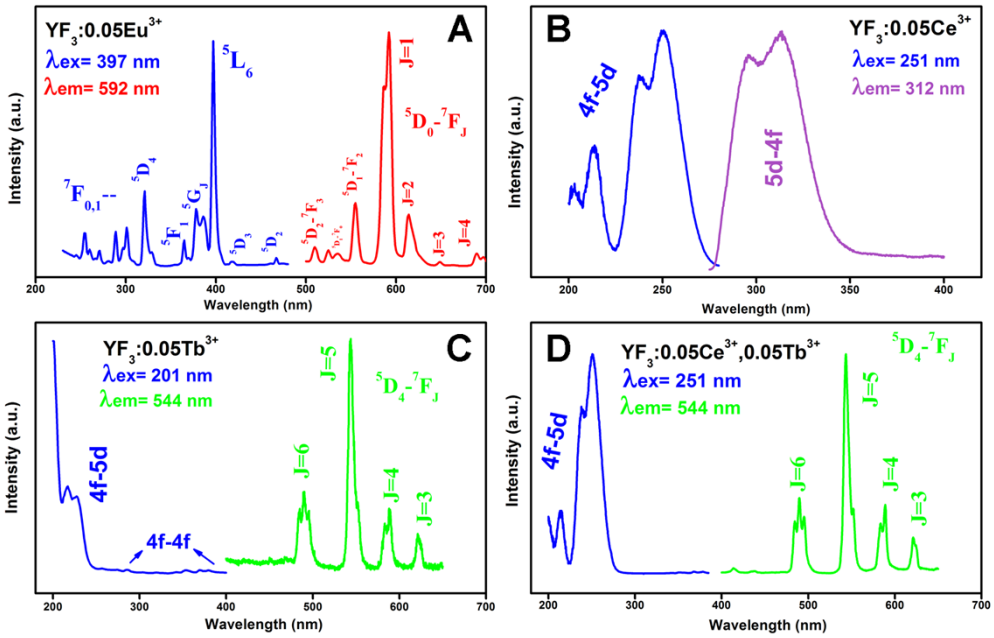

Figure S8 The excitation and emission spectra of the as-prepared (A) YF_3:0.05Eu^{3+}, (B)

YF_3:0.05Ce^{3+}, (C) YF_3:0.05Tb^{3+}, and (D) YF_3:0.05Ce^{3+},0.05Tb^{3+} products with octahedral morphology prepared with $Y(NO_3)_3$ concentration at 1 mmoL/25 mL.

The excitation spectrum of YF_3:0.05Eu^{3+} (monitored at 592 nm, $^5D_0$-$^7F_1$ transition) consists of the characteristic absorption peaks of the Eu^{3+} corresponding to the direct excitation of the ground state into excited state of 4f-electrons of the Eu^{3+} ions, which can be assigned to the $^7F_{0,1}$–$^5D_{2,3,4}$, $^7F_{0,1}$–$^5L_6$, $^7F_{0,1}$–^5G_J, and $^7F_{0,1}$–$^5F_1$ transitions of the Eu^{3+} ion, respectively. No notable band can be observed in the UV region (200-300 nm), which is owing to the high electronegativity of fluorides places the $F^- \rightarrow Eu^{3+}$ charge-transfer (CT) absorption band into the VUV region. Upon UV excitation at 397 nm, the as-obtained YF_3:Eu^{3+} products exhibit strong orange-red emission. The emission spectrum are composed of a group of characteristic lines of the Eu^{3+} ions in the range of 500-700 nm, which can be assigned to the $^5D_0$-$^7F_3$, $^5D_1$–$^7F_{0,2}$, and $^5D_0$–^7F_J (J = 1–4) transitions, respectively. The dominant emission centered at 592 nm is corresponding to the $^5D_0$–$^7F_1$ magnetic dipole transition, which should have indicated that Eu^{3+} occupies a site with inversion symmetry in the host.[1] In the YF_3:Eu^{3+} crystal structure, Y^{3+} ion is surrounded by eight F^- ions with similar distance and a ninth F^- ion with a longer distance, forming a tricapped prism.[2] Such polyhedron can be visualized to give a C_s site symmetry to Y^{3+} ion, and the noncentrosymmetry is supposed to favor the higher intensity of the $^5D_0$–$^7F_2$ forced electric dipole transition. However, for YF_3:Eu^{3+} case, the high ionicity of the Eu-F bonds allows only a little admixture of opposite parity state to the Eu^{3+} f-state, and thus the $^5D_0$–$^7F_2$ forced electric dipole transition is far less favorable.[3]

The excitation spectrum of YF_3:0.05Ce^{3+} (Figure S7B) exhibit two broad bands, one is located at 251 nm with a shoulder band centered at 237 nm, and the other is located at 213 nm with a shoulder band centered at 201 nm. The broad bands can be assigned to the parity permitted (Δl=1)

transitions from the ground state $^2F_{5/2}$ to the different components of the excited 5d state split by crystal field. The emission spectrum consists of a broad band dominated by 312 and 295 nm, which can be assigned to the transitions from the lowest 5d excited state of Ce^{3+} to the $^2F_{5/2}$ and $^2F_{7/2}$ spin-orbit components of 4f configuration. For YF_3:0.05Tb^{3+} (Figure S7C), the excitation spectrum consists of sharp band edge at 201 nm assigned to spin-allowed 4f-5d transition, and the other absorption bands before 270 nm with maximum at 217 and 227 nm corresponding to spin-forbidden 4f-5d transitions. The weak lines beyond 270 nm are electric dipolar forbidden (Δl=0) 4f-4f transitions within $4f^8$ configuration of Tb^{3+}. The emission spectrum excited at 201 nm exhibits green emissions stemming from $^5D_4$-^7F_J (J=6-3) transitions within $4f^8$ configuration of Tb^{3+}. A spectral overlap between the Ce^{3+} emission and Tb^{3+} 4f-4f transitions absorption lines can be observed, indicating a possible efficient energy transfer from Ce^{3+} to Tb^{3+}. When Ce^{3+} and Tb^{3+} were co-doped into the YF_3 host, the as-prepared YF_3:0.05Ce^{3+},0.05Tb^{3+} products exhibit intense green emissions of Tb^{3+} $^5D_4$-^7F_J (J=6-3) transitions under excitation into the Ce^{3+} absorption band (251 nm). The corresponding excitation peaks can be assigned to Ce^{3+} absorption band. Such evidences reveal the efficient Ce^{3+}-Tb^{3+} energy transfer, which has been reported in some hosts cases.[4,5]

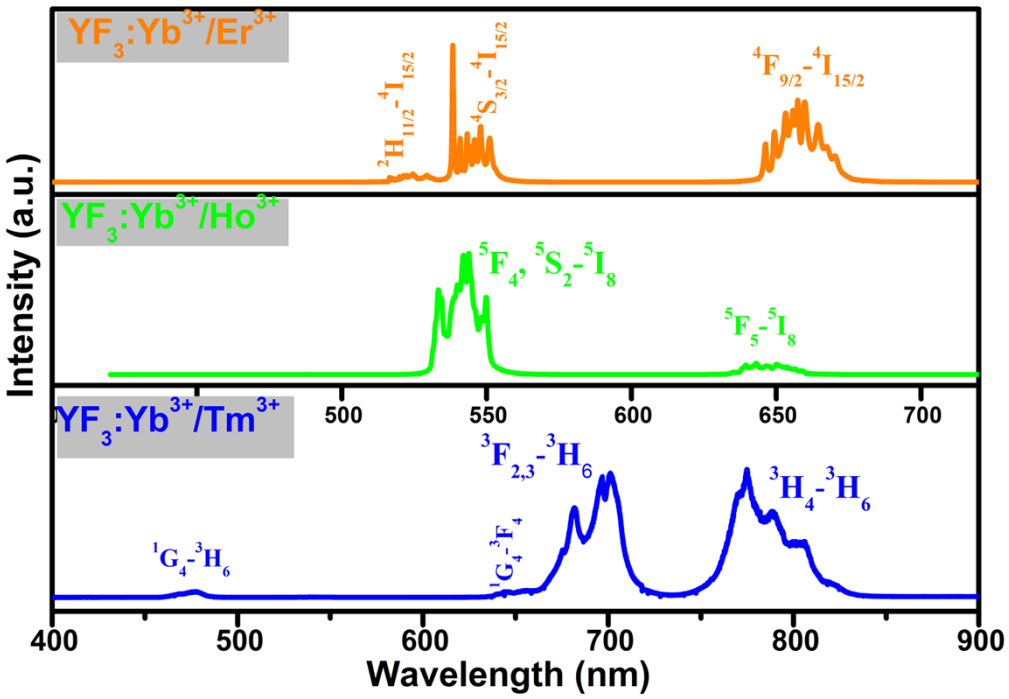

Figure S9 Up-conversion emission spectra of YF_3:0.18Yb^{3+},0.02Er^{3+}, YF_3:0.18Yb^{3+},0.02Ho^{3+}, and YF_3:0.18Yb^{3+},0.02Tm^{3+} samples with octahedral morphology excited by a 980 nm laser. All the samples were of octahedral morphology prepared with $Ln(NO_3)_3$ concentration at 1 mmoL/25 mL.

For YF_3:Yb^{3+},Er^{3+} sample, the green emission bands in the range of 515-560 nm corresponds to the $^2H_{11/2}$-$^4I_{15/2}$ and $^4S_{3/2}$-$^4I_{15/2}$ transitions of the Er^{3+} respectively, and the red emission band in the range of 635-680 nm corresponds to the $^4F_{9/2}$-$^4I_{15/2}$ of the Er^{3+} transition. For YF_3:Yb^{3+},Ho^{3+} sample, the intense green emission ranging from 529 to 560 nm comes from $^4F_4$,$^5S_2$-$^5I_8$ transition, and the relative weak $^5F_5$-$^5I_8$ transition contributes to the red emission centered at 645 nm. In the UC spectrum of YF_3:Yb^{3+},Tm^{3+} sample, the mainly emission bands in the range of 630-730 and 735-835 nm locate in the red and near infrared (NIR) regions, which can be ascribed to the $^1G_4$-$^3F_4$, $^3F_{2,4}$-$^3H_6$ (red region), and $^3H_4$-$^3H_6$ (NIR region) transitions of the Tm^{3+}, respectively. The relative weak blue emission band in the range of 460-490 nm can be ascribed to the $^1G_4$-$^3H_6$ transition of the Tm^{3+}. The corresponding UC mechanisms have been described in details in many previous reports, the green

and red UC emissions in both $YF_3:Yb^{3+},Er^{3+}$, and $YF_3:Yb^{3+},Er^{3+}$ are generated by a two-photon UC mechanism, while two- and three-phonon UC mechanisms are involved for the red and blue UC emission respectively in the $YF_3:Yb^{3+},Tm^{3+}$.[6,7]

1. B. Judd, *Phys. Rev.* 1962, **127**, 750.
2. A. Zalkin, D. Templeton, *J. Am. Chem. Soc.* 1953, **75**, 2453-2458.
3. M. M. Lezhnina, T. Jüstel, H. Kätker, D. U. Wiechert, U. H. Kynast, *Adv. Funct. Mater.* 2006, **16**, 935-942.
4. H. Meyssamy, K. Riwotzki, A. Kornowski, S. Naused and M. Haase, *Adv. Mater.*, 1999, **11**, 840-+.
5. D. Jia, R. S. Meltzer, W. M. Yen, W. Jia and X. Wang, *Appl. Phys. Lett.*, 2002, **80**, 1535-1537.
6. D. Chen, Y. Wang, Y. Yu, P. Huang, *Appl. Phys. Lett.* 2007, **91**, 251903.
7. G. Wang, W. Qin, J. Zhang, J. Zhang, C. Cao, L. Wang, G. Wei, P. Zhu, R. Kim, *J. Phys. Chem. C* 2008, **112**, 12161.